DOI: 10.1002/chem.201000589

Hydrogen Adsorption and Diffusion in *p-tert*-Butylcalix[4]arene: An Experimental and Molecular Simulation Study

Saman Alavi,*[a] Tom K. Woo,[a] Andrew Sirjoosingh,[a] Stephen Lang,[b] Igor Moudrakovski,[b] and John A. Ripmeester*[b]

Abstract: Experimental adsorption isotherms were measured and computer simulations were performed to determine the nature of the H_2 gas uptake in the low-density *p-tert*-butylcalix[4]arene (tBC) phase. ^{1}H NMR peak intensity measurements for pressures up to 175 bar were used to determine the H_2 adsorption isotherm. Weak surface adsorption (up to $\approx$2 mass% H_2) and stronger adsorption (not exceeding 0.25 mass% or one H_2 per calixarene bowl) inside the calixarene phase were detected. The latter type of adsorbed H_2 molecule has restricted motion and shows a reversible gas adsorption/desorption cycle. Pulsed field gradient (PFG) NMR pressurization/depressurization measurements were performed to study the diffusion of H_2 in the calixarene phases. Direct adsorption isotherms by exposure of the calixarene phase to pressures of H_2 gas to $\approx$60 bar are also presented, and show a maximum H_2 adsorption of 0.4 H_2 per calixarene bowl. Adsorption isotherms of H_2 in bulk tBC have been simulated using grand canonical Monte Carlo calculations in a rigid tBC framework, and yield adsorptions of $\approx$1 H_2 per calixarene bowl at saturation. Classical molecular dynamics simulations with a fully flexible calixarene molecular force field are used to determine the guest distribution and inclusion energy of the H_2 in the solid with different loadings.

Keywords: calixarenes · computational chemistry · hydrogen storage · molecular dynamics · NMR spectroscopy

Introduction

There is much interest in developing solid-state inclusion compounds for hydrogen storage.[1] The motivation is to deliver hydrogen fuel in a denser (per unit mass or volume of solid material) and safer form than cryogenically cooled liquid hydrogen or compressed gas-phase hydrogen stored in heavy walled cylinders. The requirements of hydrogen storage are different depending on the nature of the gas delivery system. For example, gas delivery to mobile car engines or hydrogen storage for residential electricity generation place very different requirements on the material used for H_2 storage. The well-known requirement that a hydrogen storage material contain $\approx$5% H_2 by mass under "reasonable" temperature and pressure conditions is appropriate for vehicles using hydrogen fuel, but a criterion based on volume of H_2 per volume of storage material may be more appropriate in gauging the performance of the material at a stationary H_2 fuel storage facility in which the fuel is not transported. In addition to the H_2 content, the temperature/pressure stability range for hydrogen storage in the material must also be taken into account.

A class of materials recently considered for hydrogen storage is the calixarenes, the most widely studied of which is *p-tert*-butylcalix[4]arene (tBC).[2] The calixarene "bowl" is composed of four *p-tert*-butylphenol units connected by methylene linkers at ortho positions to the hydroxyl groups. The low-density solid form of tBC[3] crystallizes in the monoclinic $P2_1/n$ space group,[4] and is made up of ABCD repeat units in the *b* direction of the unit cell (see Figure 1). Two adjacent calixarene bowls form a "capsule" as shown by the dashed ellipses in Figure 1, with *tert*-butyl groups en-

[a] Dr. S. Alavi, Prof. T. K. Woo, A. Sirjoosingh
Centre for Catalysis Research and Innovation
Department of Chemistry, University of Ottawa
Ottawa, Ontario K1A 6N5 (Canada)
Fax: (+1) 613-562-5179
E-mail: saman.alavi@nrc-cnrc.gc.ca

[b] Dr. S. Lang, Dr. I. Moudrakovski, Prof. J. A. Ripmeester
Steacie Institute for Molecular Sciences
National Research Council of Canada
100 Sussex Dr., Ottawa, Ontario K1A 0R6 (Canada)
Fax: (+1) 613-998-7833
E-mail: John.Ripmeester@nrc-cnrc.gc.ca

Supporting information for this article is available on the WWW under http://dx.doi.org/10.1002/chem.201000589.

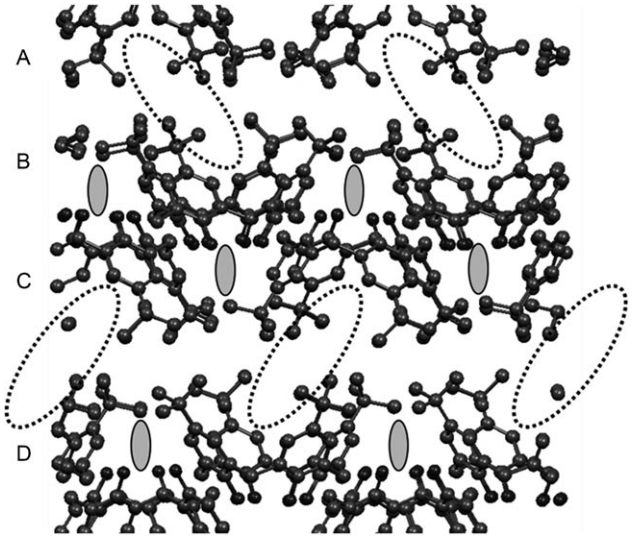

Figure 1. The low-density calixarene β_0-phase with hydrogen atoms eliminated for clarity. The four-layer ABCD repeat unit of the solid phase along the *b* direction is shown. Capsules are marked with dashed ellipses and interstitial sites with solid ellipses.

closing the central capsule region. There are four bowls per unit cell ($Z=4$). The *tert*-butyl moieties of the bowls lie between the A–B and C–D layers of the tBC structure. The closed interstitial spaces in the lattice lie between the B–C and A–D layers, and in Figure 1 are shown schematically by the solid ellipses. The low-density tBC solid phase retains its crystal morphology when reversibly adsorbing small molecules[5,6] such as Xe,[7] NO, air, SO_2, N_2, O_2, H_2, CH_4,[8] and CO_2 at low pressures, but at higher pressures the host lattice structure and solid-state space group may be modified.[7,9]

Experimentally, hydrogen forms an inclusion compound with tBC at 298 K and ≈31 bar with 66% calixarene bowl occupancy.[10] H_2 gas is known to diffuse through the solid calixarene phase. Adsorption and diffusion of guests occurs with retention of the calixarene crystal structure and without the presence of large continuous pores in the lattice, unlike the case for zeolites. Mechanisms based on the slippage of calixarene layers[12] or rotation of *tert*-butyl groups like turnstiles to direct guests through the solid[13] have been proposed to account for the diffusion of guest molecules through the calixarene structures.

We recently studied the structural and dynamical behavior of the low-density β_0-phase calixarene inclusion compound with hydrogen and other guest species using molecular dynamics simulations with guest–host occupancy ratios up to 6:1.[14] At occupancy ratios up to 1:1, the unit cell volume and inclusion energy per guest are constant.[14] At higher occupancies the unit cell volume increases, and the inclusion energy per H_2 guest decreases.[14] Daschbach et al.[15] use a potential of mean force methodology to calculate the free energy of capturing H_2 in isolated tBC bowls and closed capsules made of two adjacent bowls. The free energy of capturing H_2 was determined to be $<4.2\,kJ\,mol^{-1}$ for temperatures above 200 K.

In this work we determined the adsorption of H_2 gas in powder samples of the low-density tBC phase over a range of pressures using ^1H NMR peak intensity (0–160 bar at 293 K) and direct manometric adsorption measurements (0–60 bar at 292 K). We also used grand canonical Monte Carlo (GCMC) simulations to study the pressure and temperature dependence of the H_2 adsorption. The main goal is to determine the maximum H_2 storage capacity of low-density tBC under practical application conditions of this material. We used GCMC simulations to calculate adsorption isotherms at 273 and 293 K and pressures up to 175 bar, and study the adsorption sites of the H_2 molecules in the calixarene phase. We studied hydrogen diffusion through the calixarene lattice with NMR pulsed field gradient (PFG) measurements, rate of pressure variation in pressurization/depressurization experiments, and molecular dynamics (MD) simulations. These measurements and simulations allowed us to evaluate the potential of this material for hydrogen storage applications.

Results and Discussion

Experimental H_2 adsorption isotherms and gas diffusion: The ^1H NMR spectrum of H_2 adsorbed in the tBC at 158 bar is shown in Figure 2. The H_2 in the system appears as three peaks: a peak centered at ≈7 ppm for the excess free hydrogen in the gas phase; a broad peak with the maximum at ≈4 ppm, which is assigned to H_2 adsorbed on the surface of the calixarene phase (see below); and a low intensity Pake doublet,[16] which is assigned to H_2 adsorbed into the calixarene bowls.

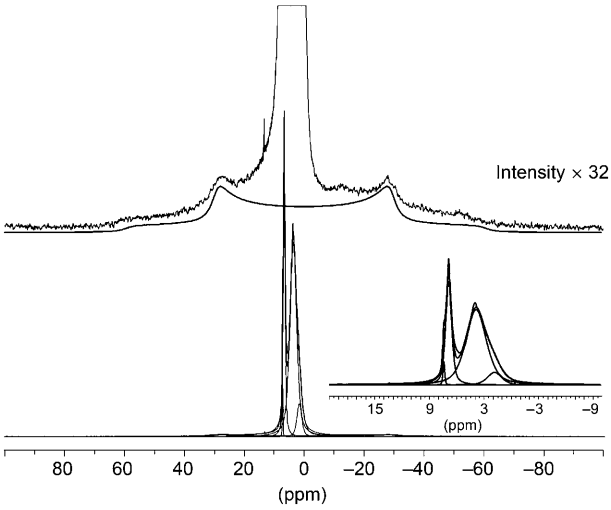

Figure 2. The NMR spectrum of the tBC phase with adsorbed H_2 in contact with excess H_2 in the gas phase at 293 K and 158 bar (the ^1H signal of tBC before H_2 adsorption has been subtracted). The inset at the top shows the spectrum with the intensity expanded 32 times. The Pake doublet of width ≈60 ppm is observed. The inset at the right shows the expanded spectrum between −5 and 15 ppm. The deconvolution of the spectrum shows the resolved peaks for the free H_2 and the weakly surface-adsorbed H_2.

The peak for the free excess H_2 gas in the presence of the solid calixarene sample is broad compared to the peak for gas-phase H_2 in a calixarene-free system. The free excess H_2 is in rapid exchange with the surface-adsorbed H_2 (4 ppm peak), and on average has a more inhomogeneous magnetic environment than the free H_2 in a calixarene-free system. The Pake doublet has a splitting of 12 kHz at 293 K, which decreases slightly with increasing temperature (between 253 and 293 K) and pressure (50 to 150 bar). This is shown in Figures S1 and S2 of the Supporting Information. Pake doublets have been observed in other systems in which H_2 is confined to small cavities,[17] for example, H_2 in fullerene shows a Pake doublet splitting of $\approx$350 kHz at $\approx$4 K,[17c] but in these cases the Pake doublet disappears at quite low temperatures (less than 10 K). As in other clathrates where molecules are confined in cages, the residual dipolar or quadrupolar couplings are determined by the anisotropic guest–host potential within the cavity.[18] Under near-room-temperature experimental conditions the hydrogen motion in the calixarene bowls is fast, but the Pake doublet shows there is still a net alignment of the H_2 molecular axes within the cavity.

The variation of the peak height with hydrogen pressure is shown in Figure S3, and the integrated peak intensities for all H_2 signals for a single run are given in Figure S4 of the Supporting Information. The total peak intensity correlates with the external H_2 pressure on the calixarene system. The integrated peak intensity of the surface-adsorbed H_2 (4 ppm peak) is considerably larger than that of the Pake doublet. The integrated peak intensities of the included H_2 guests corresponding to the Pake doublet peak at different H_2 pressures can be used to obtain an experimentally measured adsorption isotherm, which is shown in Figure 3. The experimental isotherm is the result of a number of adsorption experiments. The maximum adsorption corresponds to about 0.25 wt% of H_2 in the calixarene phase. This is equivalent to approximately one H_2 molecule per calixarene bowl. H_2 gas is a mixture of *ortho*- and *para*-H_2, with the zero-spin *para* form being invisible to the ^{1}H NMR experiment. At room temperature the *ortho*:*para* ratio is about 3:1, with conversion between the forms relatively slow. The integrated intensity of the Pake doublet therefore represents 75% of the total hydrogen strongly adsorbed.

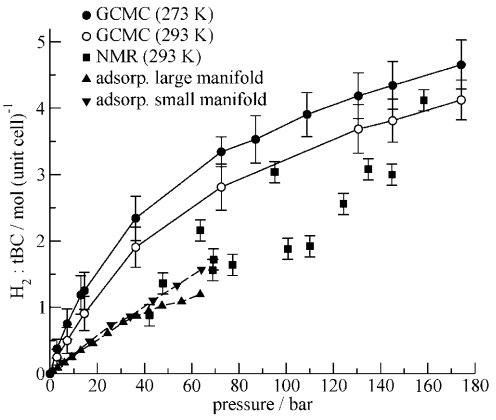

Figure 3. The experimental pressure dependence of the ^{1}H NMR intensity of the doublet signal during adsorption and desorption of H_2 in tBC at 293 K. Large experimental errors are mainly due to the uncertainties of integration in the presence of signals of vastly different intensities. Adsorption isotherm for H_2 on a 2.1 g sample of low-density tBC (▲) and on a 0.3 g sample of low-density tBC (▼) in the 3 cm^3 system. Both experiments were performed at 292.0 K. The calculated GCMC adsorptions at two temperatures are given for comparison.

Pulse field gradient (PFG) measurements were performed on the same materials to determine the diffusion coefficients of H_2 molecules making up the different peaks of the NMR spectrum. In a PFG experiment, the intensity I of the spin-echo signal attenuates with the intensity of the applied pulse field gradient G as $I \propto \exp(-\gamma^2\delta^2G^2D\Delta)$, in which γ is the proton gyromagnetic ratio, D is the self-diffusion constant, and δ and Δ are the length and the separation between the applied gradients, respectively.[19] Figure 4 shows a representative PFG experiment for H_2 in tBC at 298 K and 135 bar. Fast attenuation of the narrow signals from surface-adsorbed (4 ppm) and gas-phase H_2 (7 ppm) with the applied gradient indicates fast diffusion of those species. The intensity of the doublet signal, however, remains unaffected by the applied gradient, which implies a very limited mobility of these strongly adsorbed H_2 molecules. The observed independence of the doublet signal of the field gradients up to 1 *T*/*m* indicates that the diffusion of these species is at least an order of magnitude slower than that of the weakly adsorbed H_2 molecules.

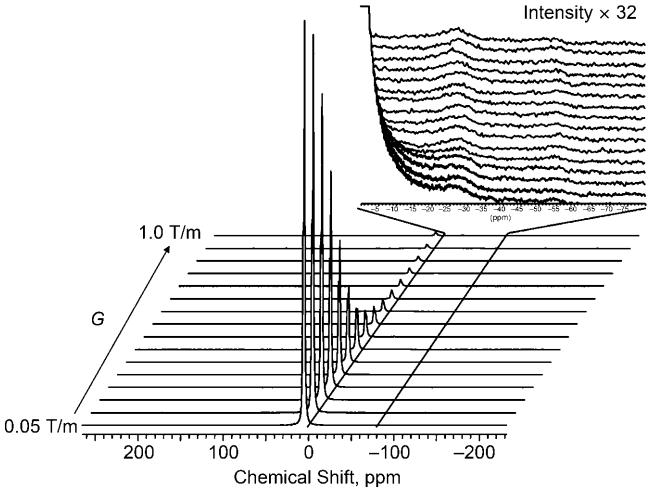

Figure 4. Variation of the ^{1}H signals for H_2 in tBC with the applied field gradient G in the PFG experiment. The upper panel shows scaled right halves of the doublet signal.

PFG-measured diffusion constants of free H_2 gas in the absence of the calixarene phase at pressures up to 145 bar are given in Figure S5 of the Supporting Information. The measured values agree well with the predictions from the mean-free-path-based simple kinetic theory of gases. The activation energy for diffusion in calixarene-free H_2 at 145 bar obtained from the variable temperature PFG experiments

was found to be 2.4 kJ mol^{-1}. Similar magnitudes of diffusion constants and an activation barrier of about 2.5 kJ mol^{-1} were previously reported for H_2 physisorbed in zeolite NaA.[19] The H_2 molecules are loosely bound in this open zeolite structure.

The temperature dependence of the diffusion coefficients for the two H_2 peaks at 7 and 4 ppm at 145 bar are shown in Figure S6 of the Supporting Information. The activation barriers to diffusion are determined to be 3.2 kJ mol^{-1} for both gas-phase H_2 in contact with the calixarene and the surface-adsorbed mobile H_2 molecules. The similarities in the magnitudes of the diffusion coefficients of H_2 in the gas phase and H_2 adsorbed on the calixarene surface indicate a rapid exchange between these two types of H_2 in the system. The slightly larger activation barrier of 3.2 kJ mol^{-1} for gas-phase H_2 in the presence of calixarene may indicate a more restricted diffusion of hydrogen molecules on the surface of tBC as compared to the open structure of the NaA.

Direct manometric measurements on calixarene powder samples at 292 K give the adsorption isotherms shown in Figure 3. The results are reasonably reproducible when performed with different samples or on different sample masses, with different dead space to sample ratios. For example, about 0.3 H_2 per cage is adsorbed at 60 bar using a 2 g sample, whereas repeating the experiment on a 0.3 g scale with a very small gas-handling manifold gave 0.35 H_2 per cage at 60 bar. The differences between the two runs are within the uncertainty margins of the manometric experiments. The H_2 equilibrates with the calixarene phase within 30 min of a pressurization/depressurization event.

Grand canonical Monte Carlo and molecular dynamics simulations: The calculated adsorption isotherms for H_2 at 273 and 293 K from GCMC calculations are shown in Figure 3. At the high pressure limit (175 bar), the predicted H_2 adsorption is found to be $\approx$4 H_2 molecules per unit cell, which is equivalent to one H_2 molecule per calixarene bowl. In porous solids such as the tBC phase studied in this work, there is a considerable amount of empty space in the simulation, in which insertion and deletion of guest molecules can occur with relatively small energy penalties. As a result, the average numbers of guests in the GCMC simulation show relatively large fluctuations, which appear as large uncertainty in the calculated isotherm. This is in contrast with the situation in GCMC simulations of dense phases, in which, after equilibration, insertion or deletion of molecules has large energy penalties, and the number of molecules in the simulation is narrowly determined.

The GCMC calculations for the adsorption isotherm at 293 K shown in Figure 3 are generally consistent with the adsorption isotherms from NMR peak intensity measurements. The NMR adsorption should be multiplied by 4/3 to give the total H_2 content (*ortho*+*para*). Both the NMR peak intensities and GCMC isotherms are higher than the low-pressure direct adsorption measurements. The GCMC calculations are performed on perfect crystals, as opposed to the real powder tBC phase samples which have imperfections and reduced adsorption sites. The adsorption of 0.2 wt% H_2 was previously measured for tBC at room temperature and 31.0 bar equilibrium pressure,[10] which roughly corresponds to a 2/3 occupancy of the calixarene bowls. This is also generally consistent with our results. The high pressure (160–170 bar) adsorption for H_2 in tBC from the NMR experiments and GCMC calculations at 293 K is between 4 and 5 H_2 per unit cell (Figure 3), which is equivalent to 1–1.2 H_2 guests per calixarene bowl. This corresponds to less than 0.5% H_2 by mass in the calixarene phase.

As mentioned in the computational methods section, the GCMC calculations are performed with a fixed tBC phase framework. Figure S7 in the Supporting Information shows that for H_2 occupancies of one per bowl, the volume of the calixarene unit cell is independent of the loading, and the assumption of a rigid framework for the calixarene phase is acceptable.

Overlaid snapshots of accepted configurations from the GCMC simulation are shown in Figure 5. Most adsorption occurs in capsules formed by two facing calixarene bowls (dashed ellipses). As seen in Figure 5, the GCMC simulations predict that, from a free energy point of view, a portion of the H_2 guests can be adsorbed into interplanar and interstitial sites. The ratio of cage to interstitial H_2 guests can be determined by assigning guests to the bowl or interstitial sites based on their position in the simulation cell from the GCMC simulations. In this work, we have not attempted to determine the spatial distribution of the H_2 guests.

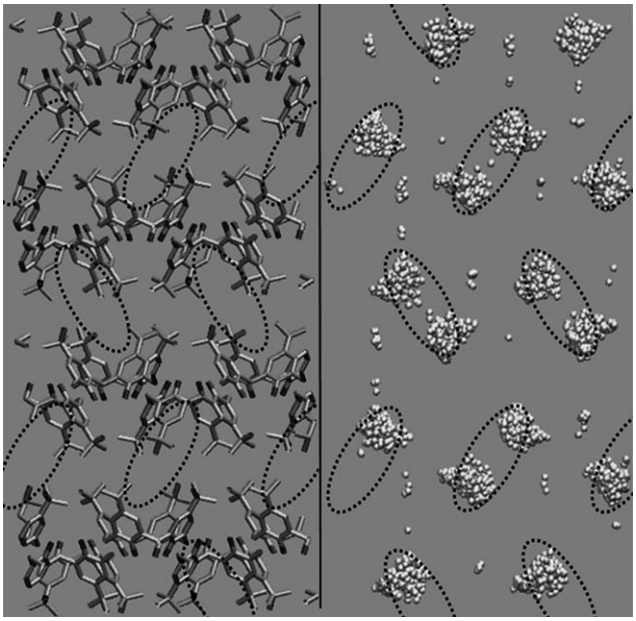

Figure 5. Overlays of accepted centre-of-mass positions of H_2 guests in the calixarene phase from GCMC calculations at 273 K and 150 bar (right). The corresponding sites in the calixarene phase (left) are shown with dashed ellipses. The occupancy at this pressure is $\approx$1 H_2 molecule per calixarene bowl.

The adsorption isobars at 1 and 100 bar pressures and different temperatures are shown in Figure 6. The low-temperature behavior is important in determining the applicability

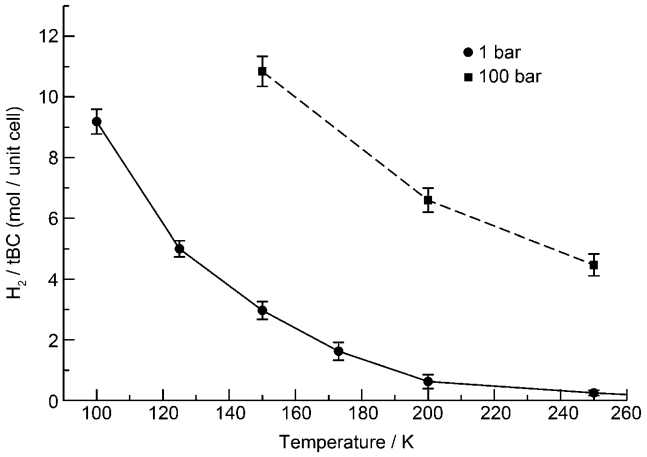

Figure 6. The H_2 uptake at different temperatures from a GCMC calculation at 1 and 100 bar.

of tBC as a hydrogen storage material for stationary sources (e.g., municipal H_2 storage). At temperatures below 200 K the H_2 storage capacity increases significantly, and occupancies of more than one H_2 guest per bowl are predicted. At lower temperatures quantum effects contribute to the behavior of the confined H_2 molecules, and the results of Figure 6 below 150 K should be considered semiquantitative. The 100 bar isobar shown in Figure 6 demonstrates that, with a combination of high pressure and low temperature, the capacity of the calixarene phase for adsorbing H_2 gas increases considerably.

Monte Carlo simulations are suitable for obtaining information on the population and distribution of guests in the solid inclusion compound under different temperature and pressure conditions. To obtain information on guest motions in the inclusion compounds, we performed molecular dynamics simulations on H_2 guests in the low-density calixarene phase. We initially placed one H_2 guest in each calixarene bowl, and MD simulations for 500 ps gave the typical hydrogen locations shown in Figure 7a. Within this timescale, the hydrogen guests remain confined to the interior of the bowls, and do not migrate into the interplanar region between the *tert*-butyl groups of adjacent A–B and C–D layers. This is consistent with the equilibrium distribution of the H_2 guests from GCMC simulations shown in Figure 6, from which it is observed that the highest probability regions for the guests are inside the calixarene bowls. Figure 7b shows snapshots of configurations from simulations in which the H_2 guest molecules were initially placed in the interstitial tBC phase sites (see Figure S8) and the system was equilibrated. In this case the H_2 guests gravitate towards the *tert*-butyl groups of the interstitial region. In the 500 ps of this simulation trajectory, some H_2 guests, circled in Figure 7b, diffuse into the calixarene bowls. Typical guest con-

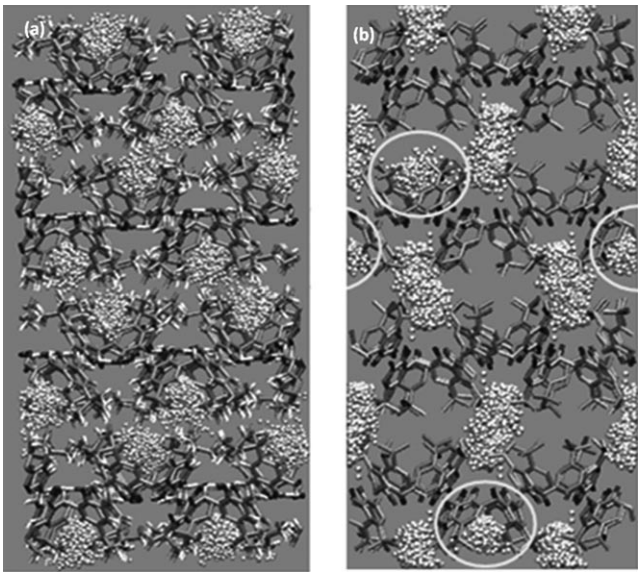

Figure 7. Overlays of snapshots from the MD simulation with one H_2 guest per calixarene bowl after 500 ps from a simulation at 273 K. Within this timeframe the H_2 molecules remain in bowls in regions adjacent to the aromatic rings of the calixarenes (left panel). Overlays of snapshots from a 100 ps MD simulation with one H_2 guest per interstitial site in the tBC phase from a simulation at 273 K (right panel). The H_2 molecules migrate from the interstitial sites towards the *tert*-butyl group in the interplanar region of the tBC phase, and some interstitial guests migrate into calixarene bowls.

figurations for a simulation beginning with three H_2 guests in each calixarene bowl are shown in Figure S9 of the Supporting Information. For these H_2 loadings, repulsions between H_2 guests push guests into the interplanar region of the tBC phase. Diffusion between different capsule sites is observed in the higher loadings.

To understand the stability of the tBC phase with different loadings, we studied the loading dependence of the simulation cell volume and the H_2 guest binding energy. The dependence of the unit cell volume on the guest occupancy at 100, 173, and 273 K and ambient pressure is shown in Figure S7 of the Supporting Information. As noted in previous work, the simulation cell volume is constant up to a loading of one H_2 per bowl, but increases sharply for larger guest occupancies. An increase of 2–10% of the unit cell volume between the empty calixarene lattice and a calixarene with a 6:1 guest:host ratio for hydrogen at different temperatures is predicted. The repulsion among the H_2 guests in the bowls leads to the expansion of the solid phase and the movement of the additional guests towards the *tert*-butyl groups in the interplanar regions of the tBC phase (see Figures S9 and S10 of the Supporting Information).

The change in configurational energy (sum of van der Waals and electrostatic energies) per H_2 guest, ΔE_{config}, is defined as given in Equation (1), in which E_{config}(calix+n guests) and E_{config}(calix) are the configurational energies per unit cell of the calixarene+guest solid phase at each occupancy and the pure β_0-phase calixarene, respectively, and n is the number of moles of guest molecules per unit cell.

$$\Delta E_{\text{config}} = [E_{\text{config}}(\text{calix} + n\,\text{guests}) - E_{\text{config}}(\text{calix})]/n \quad (1)$$

In writing Equation (1), it is assumed that H_2 is an ideal gas under the pressure/temperature conditions of the calculation. The configuration energies per H_2 guest for different occupancies of the H_2 are plotted in Figure S10 for 173 and 273 K at 1 bar pressure. The configurational energies for occupancies up to 1:1 are relatively constant at $\approx -10.5\,\text{kJ mol}^{-1}$, which shows that H_2 molecules at adjacent adsorption sites (bowls) do not interact. After 1:1 occupancy, the repulsive interactions among the H_2 guests cause a decrease in the magnitude of the configuration energy per guest. However, even up to occupancies of 6 H_2 per calixarene bowl, the configurational energies are negative ($-4.2\,\text{kJ mol}^{-1}$). The average configurational energy of one H_2 molecule in the interstitial region at 273 K is shown in Figure S10 in the Supporting Information and has a value of $-6.3\,\text{kJ mol}^{-1}$. These sites are significantly less binding than the bowl adsorption sites. From the negative configuration energies at all H_2 loadings we see that it is the unfavorable entropy effects associated with confining H_2 molecules from the gas phase into the small volume of the bowls, and not the energetic repulsions between the H_2 and bowl, that limit the hydrogen capacity of the calixarene material at low pressures.

The mean-square displacement (MSD) of H_2 molecules in a configuration with one H_2 guest in each bowl (corresponding to overlaid snapshots of Figure 7a) has been studied quantitatively with NVE molecular dynamics calculations. The MSD for the hydrogen molecules at 273 K is shown in Figure S10 in the Supporting Information. The slope of the MSD between 200 and 700 ps is $1.39\times10^{-10}\,\text{m}^2\text{s}^{-1}$. This range for the diffusion coefficient is consistent with the NMR results, which show that the diffusion of the tightly bound H_2 molecules giving rise to the Pake doublet is at least an order of magnitude lower than the $10^{-8}\,\text{m}^2\text{s}^{-1}$ observed for the diffusion coefficient of the surface-adsorbed H_2 molecules.

From Figure 7a, we expect the diffusion of the H_2 molecules between capsules in the calixarene phase to be relatively slow and to occur primarily through a hopping mechanism, in which H_2 molecules spend long time intervals inside each capsule and occasionally jump out and undergo a period of relatively fast diffusion before being captured again by another capsule. For such a hopping mechanism, the long-time behavior of the MSD will not necessarily change with time in a linear fashion.[20] The diffusion is characterized by the exponent β, as given in Equation (2).

$$\text{MSD} \propto t^{\beta} \quad (2)$$

The exponent is determined by the slope of the log-log graph of the MSD as a function of time, shown in Figure S11 of the Supporting Information. The exponent was calculated as $\beta = 0.28$, which verifies that the diffusion mechanism is not homogenous (hydrodynamic or Fickian) on this timescale. To characterize the diffusion coefficient of the H_2 guests quantitatively, long-time simulations would be needed to determine the residence time of the guests in the calixarene capsules.[21]

The different spatial distribution and diffusion mechanism of the H_2 guests at higher loadings observed in the MD simulations (Figures S9 and S10 in the Supporting Information) may suggest a loading pathway for the H_2 through the nonporous tBC phase. At the gas/tBC interface, the H_2 pressure leads to higher cage loadings and the resulting relatively fast diffusion of the H_2 guests into the interplanar regions. As the pressure equilibrates throughout the sample and each bowl is occupied by one H_2 guest, the rate of diffusion of further H_2 guests should increase significantly. A breakthrough experiment at different pressures should indicate a change in diffusion mechanisms at different occupancies.

Conclusion

The ^{1}H NMR spectrum of H_2 in the tBC phase shows a Pake doublet structure for H_2 adsorbed in the calixarene bowls. The doublet structures are stable up to room temperature, which illustrates that the H_2 interacts strongly with the conical calixarene bowl. The tBC bowl is fairly small, and confines the H_2 molecules to be aligned within a range of the bowl axis.

Variable-pressure ^{1}H NMR peak intensities and direct volumetric adsorption measurements were used to determine the experimental H_2 adsorption isotherm of tBC at 292–293 K. Grand canonical Monte Carlo and molecular dynamics simulations were used to study calixarene inclusion compounds with hydrogen guest molecules and understand the experimental results. The NMR experimental results and GCMC simulations show that at room temperature, for pressures up to 160 bar, single or double occupancy of the calixarene bowls in tBC is the stable configuration, which leads to a hydrogen storage capacity of 0.25–0.5 mass %. These values are considerably smaller than those required for mobile vehicle applications. The capacity of H_2 in the calixarene phase is $\approx$3–4 $g_{H_2} L^{-1}_{\text{calixarene}}$ in the same temperature and pressure range. The calixarene material shows improved adsorption at low temperatures and high pressures, so a combination of these conditions can be used to obtain considerably higher adsorption amounts. Furthermore, the nature of the adsorption sites and mechanism of diffusion of H_2 through the tBC material change at higher loadings (see Figure S9 in the Supporting Information), for which the magnitude of the guest–guest interactions becomes larger. This affects the applicability of this material as a hydrogen storage medium.

The Pake doublet shape from the ^{1}H NMR experiments shows that the hydrogen encapsulated in the calixarene phase has restricted motion; this is verified by PFG experiments and MD simulations. The adsorbed H_2 molecules are mostly confined to the calixarene bowls, with occasional diffusion through the *tert*-butyl into the interplanar region and into a neighboring calixarene bowl. The low mobility of the

H_2 guests suggests that they have small diffusion coefficients in this material. However, the loading of the calixarene phase and the stabilization of the NMR peak intensities and manometric H_2 adsorption values occurred in less than 20 mins.

When testing a specific material for H_2 adsorption capabilities, it is important to determine a range of pressure/temperature conditions under which the material can be used. At room temperature and pressures up to 160 bar, the low-density tBC material does not have a large H_2 storage capacity, but it can become feasible to use this material at easily accessible lower temperature and high pressure conditions.

These studies show that to improve the H_2 storage capacity of the family of calixarene materials, it is probably more effective to increase the number of aromatic groups in the structure or to add functional groups which improve the interaction with H_2 guests on the aromatic rings. The *tert*-butyl region of the calixarene is largely avoided by the H_2 guests, and so increasing the length of these alkyl chains with the idea of increasing the capsule size may not be an effective strategy for improving H_2 uptake.

Experimental Section

The low-density form of tBC was prepared by heating the commercially obtained dense form (Aldrich) to 290 °C in a vacuum-sealed Pyrex tube. X-ray structural data for the empty low-density β_0-tBC phase are given in references [3,4]. The PXRD structure of the low-density phase with H_2 guest was not obtained, but the ^{13}C CP-MAS spectra of the low-density tBC sample before and after H_2 adsorption were identical.

All NMR experiments were performed on a Bruker Avance-200 instrument in a magnetic field of 4.7 T and Larmor frequency of 200 MHz. A high-pressure NMR cell, similar in design to those previously reported,[22] coupled with a 10 mm Bruker MI2.5 microimaging probe was utilized for H_2 adsorption studies. The absolute concentration of the adsorbed H_2 species can be determined by monitoring NMR peak intensities of the guests as a function of H_2 pressure on the calixarene phase. The NMR peak intensities stabilized within 20 mins or less (see Figure S12 in the Supporting Information). Calibration of the absolute intensities of the signals was performed using samples of zeolite NaA with a known amount of interstitial water.[23] Pressure increase and decrease experiments between 0 and 160 bar (2300 psi) were performed to determine hysteresis effects in the gas adsorption/desorption process. After applying H_2 pressures to the calixarene phase, the ^1H NMR peak heights eventually stabilized to indicate equilibration of the guest H_2 in the calixarene phase. After equilibration, the ^1H NMR signal of the host calixarene phase was subtracted from the total signal to obtain the H_2 signal.

Self-diffusion of the H_2 gas in the calixarene phase was measured using the Pulsed Field Gradient (PFG) method.[24] The gradient coils used produce magnetic field gradients up to 100 Gauss cm^{-1}. To test the methodology, the self-diffusion of H_2 gas at 2105 psi was measured and compared to existing literature.

Manometric measurement of the H_2 uptake of β_0-tBC was performed using standard Sieverts' methods.[25] Two manifolds were constructed, using 316 stainless steel wherever possible. One manifold had gas reservoir and sample cell volumes of about 20 cm^3 and 12 cm^3, respectively, and required 2–3 g of tBC to detect any H_2 uptake. The other, intended for smaller sample sizes, had reservoir and cell volumes of 2 cm^3 and 1 cm^3, respectively, and could be used with about 0.2 g of sample. Pressure and temperature logging was used on both systems to aid in assessing equilibration. The samples were evacuated at room temperature at least overnight before all experiments, to a final pressure of about 2×10^{-5} torr. Expansion of helium at pressures near 1 bar from the known manifold volume was used to measure the cell volume with the sample present. H_2 was treated as non-ideal, with gas densities taken from NIST tables.[26]

A $2\times2\times2$ replica of the unit cell of the low-density calixarene β_0-phase was used in the simulation, with initial positions of the atoms in the unit cell taken from X-ray crystallography.[5] In the grand canonical Monte Carlo (GCMC) simulations, the tBC framework was frozen, with intermolecular van der Waals parameters taken from the general AMBER force field (GAFF).[27] Electrostatic point charges on atoms of tBC were assigned based on Mulliken analysis using calculations at the HF/6–31G(d) level. The H_2 molecules were considered rigid, with Lennard–Jones (LJ) parameters taken from the Wang potential.[28] Atomic point charges on the hydrogen atoms and the H_2 center of mass were assigned to reproduce the gas-phase quadrupole moment of H_2. The LJ parameters and point charges of the H_2 guest molecules are given in Table S1 of the Supporting Information. Coulombic long-range interactions were calculated using Ewald sums[29] with a precision 1×10^{-6}, and all interatomic interactions in the simulation box were calculated within a cutoff distance of $R_{cutoff}=12.0$ Å.

GCMC simulations on the system were performed with a code developed in-house, which generates H_2 guest configurations in the rigid tBC lattice at different pressures to calculate the hydrogen adsorption isotherm. Configurations of the guests in the tBC phase were sent to the DL_POLY 2.18 molecular dynamics code[30] to calculate the energy of the configuration for testing the MC acceptance criteria.[29] Trial Monte Carlo moves were generated for equal probabilities of H_2 displacement (including rotations), insertion, and deletion from the calixarene framework. After the gas content of the system was converged, gas uptake values from the GCMC calculations were taken after a total of 1.2×10^6 accepted Monte Carlo configurations.

In the molecular dynamics (MD) simulations for determining the mobility and diffusion of H_2 molecules in the tBC framework, the *p-tert*-butylcalix[4]arene molecules are considered to be fully flexible, with the intra- and intermolecular force parameters taken from GAFF. Details of the AMBER force field used to describe the tBC molecules are given in the Supporting Information. Equilibrium molecular dynamics simulations of the inclusion compounds were calculated with an H_2 guest loading of one per bowl with isotropic constant pressure, constant temperature (NpT) ensemble molecular dynamics simulations with DL_POLY 2.18. The Nosé–Hoover thermostat–barostat algorithm,[31] with thermostat and barostat relaxation times chosen as 0.1 and 1.0 ps, respectively, was used to maintain the temperature and pressure of the systems. The equations of motion were integrated with a time step of 0.5 fs using the Verlet leap-frog scheme.[27] The H_2 molecules were placed randomly in the calixarene phase and the simulation cells were annealed with a minimum of two 100 ps equilibration/simulation cycles until a convergence of 1% or better in the total energy was obtained. Five NVE trajectories of 1.5 ns at 2105 psi and 273 K temperature were performed to study the H_2 guest diffusion in the tBC phase.

Acknowledgements

This work was partly supported by the Saga Prefecture of Japan as part of a collaborative Research and Development project. We would like to thank Dr. Hajime Endou of Technova Inc. (Tokyo, Japan) for facilitating the collaborative project. S.A., T.K.W. and A.S. gratefully acknowledge the Canada Research Chairs Program and the Natural Sciences and Engineering Research Council of Canada (NSERC) for financial support. The support of the National Research Council of Canada is also acknowledged.

[1] a) A. Züttel, *Mater. Today* **2003**, *6*, 24–33; b) H. Frost, R. Q. Snurr, *J. Phys. Chem. C* **2007**, *111*, 18794–18803; c) L. Zhou, *Renewable Sustainable Energy Rev.* **2005**, *9*, 395–408.
[2] a) *Calixarenes 2001* (Eds.: M. Z. Asfari, V. Böhmer, J. Harrowfield, J. Vicens), Kluwer, New York, **2001**; b) J. A. Ripmeester, G. A. Enright, C. I. Ratcliffe, K. A. Udachin, I. L. Moudrakovski, *Chem. Commun.* **2006**, 4986–4996; c) C. D. Gutsche, *Calixarenes: An Introduction*, RSC, London, **2008**; d) W. Śliwa, C. Kozłowski, *Calixarenes and Resorcinarenes: Synthesis Properties and Applications*, Wiley-VCH, Weinheim, **2009**.
[3] E. B. Brouwer, G. D. Enright, K. A. Udachin, S. Lang, K. J. Ooms, P. A. Halchuk, J. A. Ripmeester, *Chem. Commun.* **2003**, 1416–1417.
[4] a) J. L. Atwood, L. J. Barbour, A. Jerga, B. L. Schottel, *Science* **2002**, *298*, 1000–1002; b) J. L. Atwood, L. J. Barbour, G. O. Lloyd, P. K. Thallapally, *Chem. Commun.* **2004**, 922–924.
[5] G. D. Enright, K. A. Udachin, I. L Moudrakovski, J. A. Ripmeester, *J. Am. Chem. Soc.* **2003**, *125*, 9896–9897.
[6] J. L. Atwood, L. J. Barbour, A. Jerga, *Angew. Chem.* **2004**, *116*, 3008–3010; *Angew. Chem. Int. Ed.* **2004**, *43*, 2948–2950.
[7] D. H. Brouwer, I. L. Moudrakovski, K. A. Udachin, G. D. Enright, J. A. Ripmeester, *Cryst. Growth Des.* **2008**, *8*, 1878–1885.
[8] P. K. Thallapally, T. B. Wirsig, L. J. Barbour, J. L. Atwood, *Chem. Commun.* **2005**, 4420–4422.
[9] K. A. Udachin, I. L. Moudrakovski, G. D. Enright, C. I. Ratcliffe, J. A. Ripmeester, *Phys. Chem. Chem. Phys.* **2008**, *10*, 4636–4643.
[10] P. K. Thallapally, G. O. Llyod, T. B. Wirsig, M. W. Bredenkamp, J. L. Atwood, L. J. Barbour, *Chem. Commun.* **2005**, 5272–5274.
[11] X. Gu, L. Zhang, X. Gong, W. M. Lau, Z. F. Liu, *J. Phys. Chem. B* **2008**, *112*, 14851–14856.
[12] G. D. Enright, E. B. Brouwer, P. Halchuk, K. Ooms, M. J. Ferguson, K. A. Udachin, J. A. Ripmeester, *Acta Crystallogr. Sect. A* **2002**, *58*, c310.
[13] G. S. Ananchenko, K. A. Udachin, M. Pojarova, S. Jebors, A. W. Coleman, J. A. Ripmeester, *Chem. Commun.* **2007**, 707–709.
[14] a) S. Alavi, N. A. Afagh, J. A. Ripmeester, D. L. Thompson, *Chem. Eur. J.* **2006**, *12*, 5231–5237; b) S. Alavi, J. A. Ripmeester, *Chem. Eur. J.* **2008**, *14*, 1965–1971.
[15] J. L. Daschbach, P. K. Thallapally, J. L. Atwood, P. McGrail, L. X. Dang, *J. Chem. Phys.* **2007**, *127*, 104703–1–104703–4.
[16] G. E. Pake, *J. Chem. Phys.* **1948**, *16*, 327–331.
[17] a) T. Su, S. Chen, P. C. Taylor, R. S. Crandall, A. H. Mahan, *Phys. Rev. B* **2000**, *62*, 12849–12858; b) L. Senadheera, M. S. Conradi, *J. Phys. Chem. B* **2007**, *111*, 12097–12102; c) M. Carravetta, O. G. Johannessen, M. H. Levitt, I. Heinmaa, R. Stern, A. Samoson, A. J. Horsewill, Y. Murata, K. Komatsu, *J. Chem. Phys.* **2006**, *124*, 104507.
[18] M. J. Collins, C. I. Ratcliffe, J. A. Ripmeester, *J. Phys. Chem.* **1990**, *94*, 157–162.
[19] E. O. Stejskal, J. E. Tanner, *J. Chem. Phys.* **1965**, *42*, 288–292.
[20] B. Smit, T. L. M. Maesen, *Chem. Rev.* **2009**, *109*, 4125–4184.
[21] a) F. Jousse, S. M. Auerbach, D. P. Vercauteren, *J. Chem. Phys.* **2000**, *112*, 1531–1540; b) S. M. Auerbach, F. Jousse, D. P. Vercauteren in *Computer Modelling of Microporous Materials*, (Eds.: C. R. A. Catlow, R. A. van Santen, B. Smit), Elsevier, Amsterdam, **2004**, pp. 49–108.
[22] a) I. T. Horváth, E. C. Ponce, *Rev Sci. Instrum.* **1991**, *62*, 1104–1105; b) I. L. Moudrakovski, G. E. McLaurin, C. I. Ratcliffe, J. A. Ripmeester, *J. Phys. Chem. B* **2004**, *108*, 17591–17595.
[23] N.-K. Bär, H. Ernst, H. Jobic, J. Kärger, *Magn. Reson. Chem.* **1999**, *37*, S79-S83.
[24] F. Stallmach, P. Galvosas, *Annu. Rep. NMR Spectrosc.* **2006**, *44*, 51–131.
[25] a) A. Sieverts, *Z. Phys. Chem.* **1914**, *88*, 451; b) T. P. Blach, E. M. Gray, *J. Alloys Compd.* **2006**, *404–424*, 692–697.
[26] E. W. Lemmon, M. O. McLinden and D. G. Friend, *Thermophysical Properties of Fluid Systems in NIST Chemistry WebBook, NIST Standard Reference Database Number 69* (Eds.: P. J. Linstrom, W. G. Mallard, National Institute of Standards and Technology, Gaithersburg **2009**, p. 20899; http://webbook.nist.gov (retrieved March, 2009).
[27] W. D. Cornell, P. Cieplak, C. L. Bayly, I. R. Gould, K. M. Merz, Jr., D. M. Ferguson, D. C. Spellmeyer, T. Fox, J. W. Caldwell, P. A. Kollman, *J. Am. Chem. Soc.* **1995**, *117*, 5179–5197. See also: http://amber.scripps.edu.
[28] W. F. Wang, *J. Quant. Spectrosc. Radiat. Transfer* **2003**, *76*, 23–30.
[29] a) D. Frenkel, B. Smit, *Understanding Molecular Simulation*, 2nd ed., Academic Press, San Diego, **2000**; b) M. P. Allen, D. J. Tildesley, *Computer Simulation of Liquids*, Oxford Science Publications, Oxford, **1987**.
[30] DL_POLY 2.18, T. R. Forester, W. Smith, CCLRC, Daresbury Laboratory, **1995**.
[31] a) S. Nosé, *J. Chem. Phys.* **1984**, *81*, 511–519; b) W. G. Hoover, *Phys. Rev. A* **1985**, *31*, 1695–1697; c) S. Melchionna, G. Ciccotti, B. L. Holian, *Mol. Phys.* **1993**, *78*, 533–544.

Received: March 6, 2010
Published online: September 1, 2010

